Title

A real-time analysis of protein transport via the twin arginine translocation pathway in response to different components of the protonmotive force

Journal

Journal of Biological Chemistry, 299(11)

ISSN

0021-9258

Authors

Zhou, Wenjie

Hao, Binhan

Bricker, Terry M

et al.

Publication Date

2023-11-01

DOI

10.1016/j.jbc.2023.105286

Peer reviewed

A real-time analysis of protein transport *via* the twin arginine translocation pathway in response to different components of the protonmotive force

Received for publication, July 17, 2023, and in revised form, August 28, 2023 Published, Papers in Press, September 22, 2023,
https://doi.org/10.1016/j.jbc.2023.105286

Wenjie Zhou[1,‡], **Binhan Hao**[1,‡], **Terry M. Bricker**[2], **and Steven M. Theg**[1,*]

From the [1]*Department of Plant Biology, University of California, Davis, California, USA;* [2]*Department of Biological Sciences, Louisiana State University, Baton Rouge, Louisiana, USA*

Reviewed by members of the JBC Editorial Board. Edited by Karen Fleming

The twin arginine translocation (Tat) pathway transports folded protein across the cytoplasmic membrane in bacteria, archaea, and across the thylakoid membrane in plants as well as the inner membrane in some mitochondria. In plant chloroplasts, the Tat pathway utilizes the protonmotive force (PMF) to drive protein translocation. However, in bacteria, it has been shown that Tat transport depends only on the transmembrane electrical potential (Δψ) component of PMF *in vitro*. To investigate the comprehensive PMF requirement in *Escherichia coli*, we have developed the first real-time assay to monitor Tat transport utilizing the NanoLuc Binary Technology in *E. coli* spheroplasts. This luminescence assay allows for continuous monitoring of Tat transport with high-resolution, making it possible to observe subtle changes in transport in response to different treatments. By applying the NanoLuc assay, we report that, under acidic conditions (pH = 6.3), ΔpH, in addition to Δψ, contributes energetically to Tat transport *in vivo* in *E. coli* spheroplasts. These results provide novel insight into the mechanism of energy utilization by the Tat pathway.

The twin arginine translocation (Tat) pathway, which is present in bacteria, archaea, thylakoids in chloroplasts, and some mitochondria, transports proteins in their folded conformation across energy-transducing membranes. This pathway plays a critical role in a variety of biosynthetic pathways, including energy metabolism, heavy metal resistance, cell division, virulence in prokaryotes, as well as photosynthesis in chloroplasts, bacteria, and cyanobacteria (1–5). The minimal Tat translocon consists of the TatA and TatC proteins, although in most systems, and TatB is also required (1, 6, 7). Transport *via* the Tat pathway is dependent on the protonmotive force (PMF), which is composed of the transmembrane electrical potential (Δψ) and proton gradient (ΔpH) (2, 8–10). However, how Tat protein transport is coupled energetically with to the PMF is unclear.

A detailed mechanistic understanding of the Tat transport mechanism is limited by current Tat transport assays. Previously, Tat transport has been investigated quantitatively in bacteria either using pulse-chase experiments *in vivo* (11) or using an inverted membrane vesicle (IMV) transport system *in vitro* (12). Both methods are labor-intensive procedures since protein samples must be obtained over a time course, followed by SDS-PAGE and autoradiography or immunoblotting. Additionally, such assays can only achieve a discontinuous monitoring of Tat transport over relatively large time intervals (mins); the acquisition of transport kinetics relying on fitting the time-course data with regression models. While such assays are sufficient for many issues, they are not well-suited for more advanced and comprehensive analyses, especially for monitoring rapid responses to different experimental conditions. Alternative procedures to investigate Tat transport have been proposed by quantifying the fluorescence of the GFP bearing a Tat signal sequence. However, these studies were also performed with discontinuous measurements, GFP fluorescence either being quantified as end points using a photon-counting spectrophotometer (13, 14), or by flow cytometry (15). Additionally, it is difficult to distinguish the fluorescence generated from the GFP precursor in the cytoplasm *versus* the mature GFP in the periplasm without further experimentation. Also, change of the cellular conformation such as formation of cell chains due to the defect in transporting the Tat substrates AmiA and AmiC (16) affects the quantitation of the GFP fluorescence measurement. Finally, transport of a completely alien substrate like GFP with a signal peptide from a Tat substrate may not reflect the Tat transport process using native cargo proteins. Thus, in order to address the limitations of the current transport assays and to conduct a more detailed analysis of Tat transport, it would be advantageous to develop a versatile, sensitive, and real-time Tat transport assay.

Recently, NanoLuc, a novel bioluminescence platform, has been developed and widely used for high-resolution imaging and other biological applications (17). Hallmarks of this system include its high stability, luminescence specificity and efficiency, and ATP-independence. Initially tailored for the study of protein-protein interactions, NanoLuc has been engineered to be split into two complementary components. The NanoLuc luciferase binary reporter system (NanoLuc Binary Technology, [NanoBiT]) (18) uses a small fragment, pep86 (1.3 kD, trademark name HiBiT), which interacts with the large

‡ These authors contributed equally to this work.
* For correspondence: Steven M. Theg, smtheg@ucdavis.edu.

component, 11S (18 kD, trademark name LgBiT), to generate a functional protein that luminesces with high intensity at 460 nm in the presence of its substrate furimazine (17). This NanoBiT system has a number of attractive features suggesting its utility for the development of a real-time Tat transport assay. First, previous studies have utilized the NanoBiT system to investigate protein secretion and transport in both mammalian cells and bacteria, both *in vivo* and *in vitro* (19–22). Second, in contrast to common split-luciferase systems which often require the presence of cofactors in addition to their substrate to produce luminescence, NanoBiT only requires molecular oxygen and its substrate furimazine to generate bioluminescence (17). This can minimize the potential interference of other reagents with the systems under investigation. Third, the rapid spontaneous interaction between the pep86-tagged Tat substrate and the 11S component (K_d of 0.7×10^{-9} M) generates luminescence allowing for the real-time monitoring of these two components in the same compartment (18). Finally, the enzymatic amplification of the luminescence signals by NanoLuc increases the sensitivity of the measurement (18), making it feasible to observe subtle changes upon different experimental treatments.

The Collinson group has exploited these properties utilizing the NanoBiT system to investigate protein transport *via* the Sec pathway in *Escherichia coli* and protein import in the mitochondria (19, 21–23). In contrast to the Tat pathway, which transports folded proteins in an ATP-independent manner, the Sec and mitochondrial pathways transport proteins in their extended, unfolded conformations in an ATP-dependent manner (24). The NanoBiT system has allowed this group to measure elementary steps in protein export or import *via* the Sec pathway in bacteria (19) or the TOM–TIM machinery in mitochondria (22).

In this study, we have used NanoBiT technology to investigate transport *via* the Tat pathway. An *in vivo* NanoBiT–based real-time protein transport assay is reported using *E. coli* spheroplasts. Upon the validation of the Tat NanoLuc transport assay, we applied it to investigate the energetics of Tat transport in bacteria by monitoring the real-time response of the transport signal to dissipation of different components of the PMF.

Results

Establishment of an in vivo *real-time transport assay for the Tat pathway in* E. coli

In order to develop a bioluminescence–based real-time assay using the NanoBiT system, we needed to transport a pep86-tagged Tat substrate into the compartment containing the 11S portion of the luciferase on the *trans*-side of the *E. coli* inner membrane (Fig. 1*A*). Since the 11S polypeptide does not freely cross the bacterial outer membrane, we established the NanoLuc assay in spheroplasts, with the outer membrane having been removed. Protein transport in spheroplasts has been studied previously (25, 26), establishing a precedent for this approach. We attached the small fragment of the luciferase, pep86, to either the N or C termini of SufI (designated Npep86-SufI or SufI-Cpep86, respectively), a well-characterized bacterial Tat substrate (11, 27) (Fig. 1*B*), and placed them under the control of T5-lacO promoter, which can be induced by the addition of IPTG. We then screened these pep86-tagged SufI constructs to determine their suitability for the transport assay. A conventional *in vivo* transport assay (28) was carried out to evaluate the performance of both pep86 variants by isolating the periplasmic fraction of cells coexpressing either WT TatABC (*i.e.*, wtTat) or *ΔtatA*, together with SufI, SufI-Cpep86, or Npep86-SufI, followed by SDS-PAGE and immunoblotting (Fig. 1, *D* and *E*). Cells with the WT Tat expressing either SufI-Cpep86 or Npep86-SufI achieved about 50% of transport relative to the WT Tat system transporting non-pep86-tagged SufI (Fig. 1*D*). As a negative control, no detectable transport of SufI, SufI-Cpep86, nor Npep86-SufI was seen with the *ΔtatA* mutant, as TatA is an essential component of a functional Tat translocon. These results indicate that attachment of pep86 at either the N terminus or C terminus of SufI still allows for SufI to retain significant transport activity relative to native SufI.

Next, we evaluated the level of overall protein induction by examining the total cell extract for each mutant. Cells expressing SufI-Cpep86 had a similar level of precursor production as the cells expressing native SufI. The abundance of Npep86-SufI, however, was significantly lower; approximately 1% relative to the level of SufI or SufI-Cpep86 (Fig. 1*E*). It is possible that either the expression or the stability of the Npep86-SufI is negatively affected. Accordingly, SufI-Cpep86 was chosen as the most suitable substrate variant to investigate Tat transport *via* the NanoLuc system, as its transportability and overall expression level most closely resembles native SufI. Consequently, the following experiments were conducted using the cells expressing and transporting SufI-Cpep86.

To set up the luminescence assay, we combined spheroplasts, purified overexpressed 11S (Fig. 1*C*), and the NanoLuc substrate furimazine in the reaction medium. Upon the addition of IPTG, transcription and subsequent translation of the SufI-Cpep86 construct was induced. When this Tat substrate was transported out of the spheroplasts across the cytoplasmic membrane into the external environment (*i.e.*, 1× $M9^+$ medium, which is the equivalent of periplasm), it came into contact with 11S, forming the active NanoLuc (11S-pep86 complex). Accompanied by the presence of furimazine and O_2, it produced luminescence, which was monitored throughout the experimental time course (Fig. 2*A*).

The in vivo *Tat NanoLuc transport assay faithfully reports Tat transport in spheroplasts*

Next, we examined SufI-Cpep86 transport in spheroplasts of wtTat and the Tat-deficient mutant *ΔtatA* to confirm that the luminescence data correctly reflects Tat transport. Upon induction with IPTG followed by ∼2 min of lag time required for transcription and translation, a continuous increase in the luminescence signal for the wtTat spheroplasts was observed (Fig. 2*A*). No significant increase in the luminescence signal

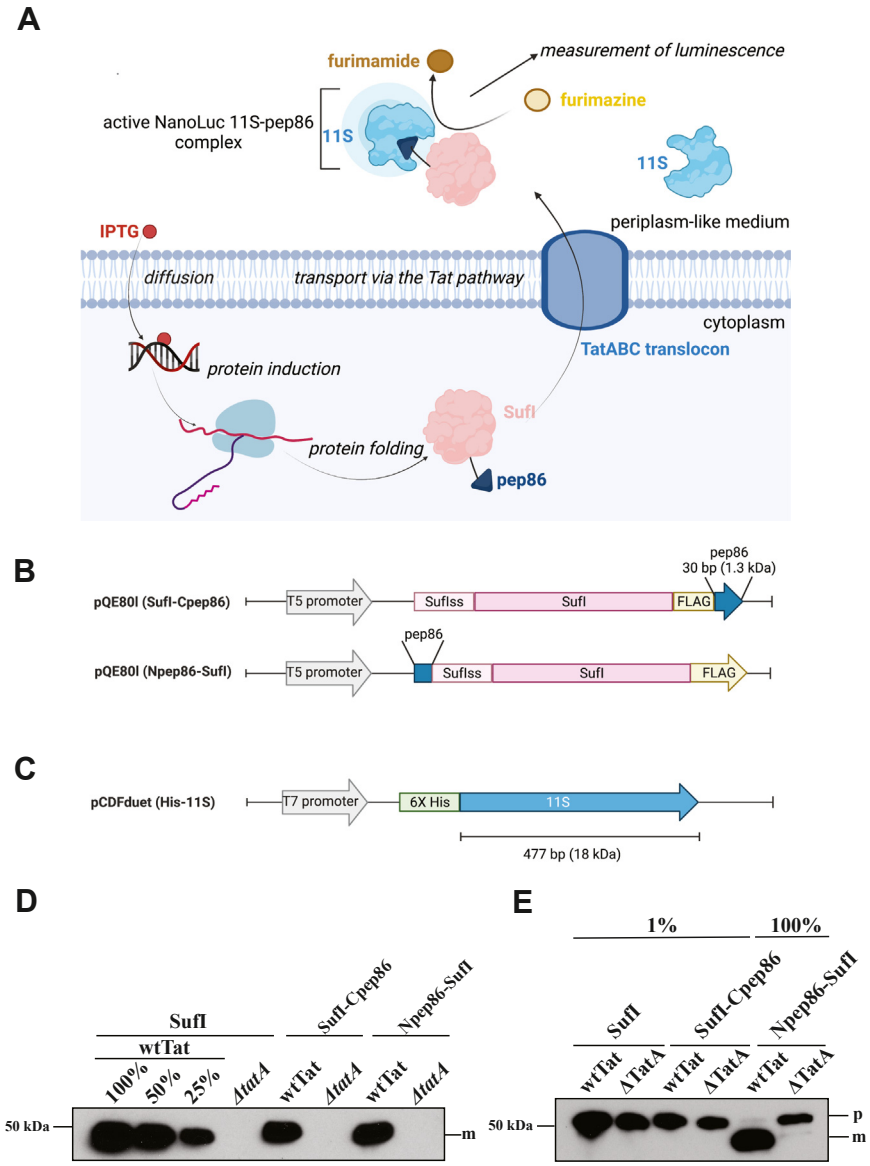

Figure 1. Schematic of *in vivo* Tat NanoLuc transport assay, and design of the pep86-variant selection. *A*, diagram explaining the experimental design of the NanoLuc transport assay. *B*, gene diagram for the pep86-tagged SufI variant. pep86 was added either at the N terminus (*i.e.*, Npep86-SufI) or C terminus (*i.e.*, SufI-Cpep86) of the SufI. *C*, gene diagram for the 11S construct. A 6× His tag was added at the N terminus for protein purification. *D*, assessment of the Tat transport activity among SufI-pep86 variants and native SufI. Periplasmic fractions from the *in vivo* transport assay were subjected to immunoblotting. *E*, assessment of the protein induction levels of the SufI-pep86 variants and native SufI. One percentage of the total extract of the cells expressing native SufI or SufI-Cpep86 is shown in lanes 1 to 4, and 100% of the total extract of the cells expressing Npep86-SufI is shown in lanes 5 and 6. Position of the 50 kDa molecular weight marker is shown to the left; p, precursor; m, mature. Tat, twin arginine translocation.

was observed with the *ΔtatA* spheroplasts. To validate that the increase in luminescence corresponded to Tat transport, the periplasmic-mimetic external medium was cleared of spheroplasts by centrifugation and subsequently subjected to SDS-PAGE and immunoblotting. No mature SufI-Cpep86 was observed in the sample collected 1 min after IPTG induction. Mature SufI-Cpep86 was observed after 20 min in wtTat spheroplasts, whereas no mature protein was observed after 20 min induction in *ΔtatA* spheroplasts. Such results are consistent with the observed NanoLuc luminescence. Additionally, the amount of SufI-Cpep86 precursor induced was similar in the total cell extracts of the wtTat and *ΔtatA* spheroplasts, which indicates that the difference in the luminescence signal between the wtTat and *ΔtatA* spheroplasts was due to a difference in transport rather than the lack of SufI-Cpep86 production in the absence of TatA (Fig. 2*A*). Notably, a very small fraction of precursor was present in the periplasmic samples from the *ΔtatA* spheroplasts. Previous studies have reported that, due to the absence of the Tat activity, *ΔtatA* spheroplasts are more susceptible to lysis compared to the wtTat cells (29). Nevertheless, the amount of precursor present in the external medium is quite small and negligible relative to the total amount of precursor synthesized (Fig. 2*A*).

In addition to confirming that the NanoLuc luminescence measurement records the SufI transport kinetics in a Tat-

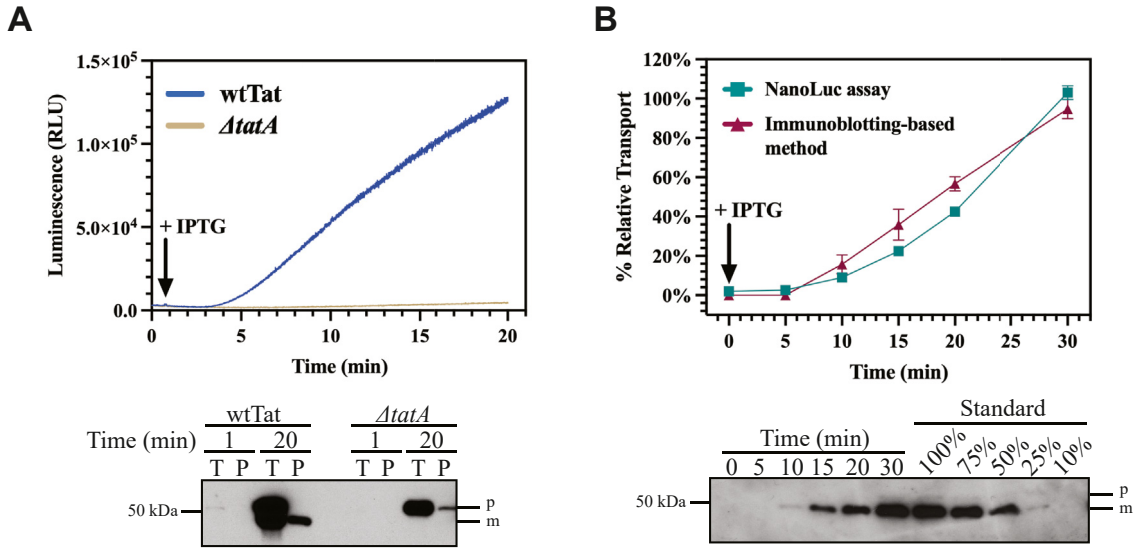

Figure 2. The NanoLuc assay gives a genuine measure of Tat transport. *A*, the NanoLuc assay correctly reports Tat-specific transport. wtTat transporting SufI-Cpep86 as the positive control (*red curve*); *ΔtatA* is shown as the negative control (*blue curve*). *Arrow* indicates the time when IPTG was added to the protein induction. Lower panel: samples were taken from the reaction cuvette after either 1 or 20 min from the reaction cuvette and immunoblotted using an antiFLAG-tag antibody. *B*, the NanoLuc assay yields results consistent with the conventional immunoblotting-based method. Standard curve is generated using the dilution series in the blot. Transport is normalized based on the level of transport at 30 min (100%) using the standard curves. Error bars indicate standard error from three replicates; a representative immunoblot is shown in the *lower panel*. RLU, relative light units; p, precursor; m, mature; Tat, twin arginine translocation. Other details as in Figure 1.

specific manner, we evaluated the consistency between the kinetic curves obtained from the luminescence assay and those from the conventional immunoblotting-based method. Three technical replicates were performed to assess the reproducibility of the NanoLuc assay. Upon IPTG induction, samples were removed at six different time points, 0, 5, 10, 15, 20, and 30 min post-IPTG induction. For the luminescence assay measurement, the corresponding luminescence readings were recorded from these samples (Fig. 2*B*). For the conventional method, samples were collected at the same time points and placed on ice to stop transport. These samples were then subjected to SDS-PAGE followed by immunoblotting, and the transport kinetics were analyzed (Fig. 2*B*). These results demonstrated that the kinetic curves obtained from the luminescence assay fully recapitulated those obtained from the conventional immunoblotting-based method. In addition to this consistency, the NanoLuc assay exhibits the following merits. First, the variation among replicates in NanoLuc assay is relatively small compared to the conventional method, yielding measurements with higher resolution. In this case, the luminescence assay allows us to identify small but significant differences in transport between different experimental treatments. Second, the luminescence measurement in the NanoLuc assay is in real time, which can minimize the experimental errors during sample handling. For example, it is observed that the percentages of transport relative to the end point were higher using the conventional method relative to the luminescence assay. Such overestimation of the transport was perhaps due to inefficient quenching of the transport process by ice, a problem rendered moot in the real-time NanoLuc assay.

Taken together, our results indicate that the NanoLuc assay is a legitimate measure of Tat transport activity that is continuous, exhibits high resolution and reproducibility, and which is therefore a suitable method for comprehensively investigating the Tat transport kinetics described in the forthcoming section and in future studies.

Investigation of the PMF dependency of the Tat machinery in E. coli *spheroplasts*

The Tat transport pathway was originally discovered in thylakoids in part based on its requirement for a ΔpH and lack of requirement for ATP to power protein transport (30). While valinomycin was initially observed to be without effect on the protein transport, an effect of the Δψ was ultimately observed under limiting light intensity, indicating that in thylakoids the Tat pathway was powered by both components of the PMF (8). Bageshwar and Musser studied the energy requirement for Tat transport into IMVs derived from *E. coli* and concluded that it was driven by the Δψ only, with no contribution from a ΔpH (12). We thought it was unlikely that two different mechanisms governed the same transport process in different organisms and recognized that our newly developed real-time luminescence assay afforded us the opportunity to revisit this question.

With these considerations in mind, we applied the NanoLuc assay to investigate Tat transport energetics in spheroplasts with respect to the different components of the PMF. First, we examined the response to collapse of the Δψ by the addition of 1 to 2 μM valinomycin (V) (Fig. 3*A*). As expected, the transport-reporting luminescence curves plateaued after valinomycin addition, while the positive control in which only the solvent ethanol was added (E) continued to increase unabated. This is consistent with the known requirement for the Δψ for Tat transport in *E. coli*. We next observed that addition of 1 to

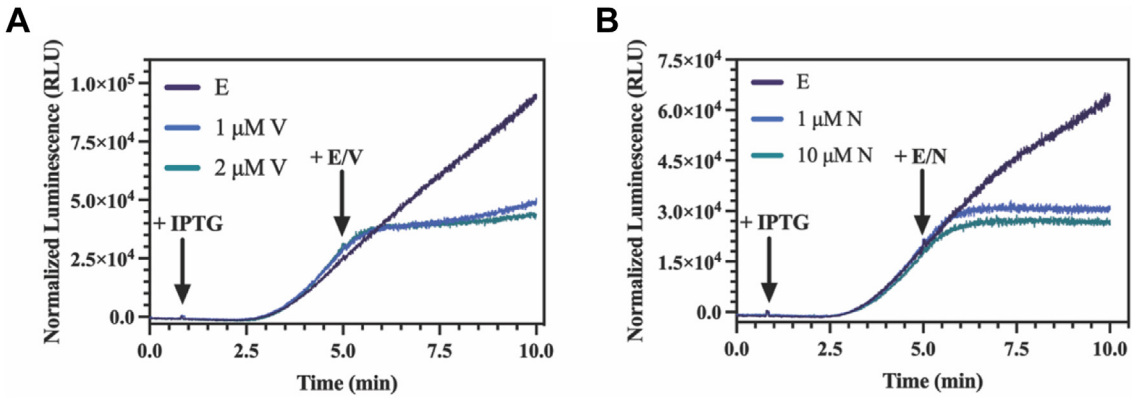

Figure 3. Both ΔpH and Δψ appear to play a role in Tat transport in *Escherichia coli* spheroplasts. Transport curves with SufI-Cpep86 in *E. coli* spheroplasts are shown. A background signal was calculated by averaging the luminescence before IPTG addition, and this background is subtracted from the luminescence signals. IPTG was added at the first arrow, ionophores (valinomycin (V, panel *A*), or nigericin (N, panel *B*)) or their solvent (ethanol (E)) were added at the second arrow. Experiments were performed at pH = 6.3. Other details as in Figure 2. Tat, twin arginine translocation.

10 μM nigericin also caused the rising luminescent signal to plateau (Fig. 3*B*), suggesting that, as in thylakoids, the ΔpH also was able to drive protein transport. This finding differed from the conclusions reached earlier in which nigericin was not observed to inhibit Tat transport in IMVs (12).

To further investigate our discrepant result, we examined several artefacts that could potentially result in the loss of the increasing NanoLuc signal upon addition of nigericin or valinomycin. First, it is possible that nigericin and/or valinomycin, themselves, could negatively impact the 11S-pep86 interaction and, consequently, affect the NanoLuc signal (21). To assess this possibility, we examined the direct effect of nigericin and valinomycin on the 11S-SufI-Cpep86 interaction. To this end, excess purified 11S and furimazine were placed in 1× $M9^+$ medium (without *E. coli* spheroplasts) and SufI-Cpep86 was added at t = 20 s to initiate the NanoLuc luminescence reaction. When the luminescence signal reached the maximum (∼160 s), ethanol, valinomycin, or nigericin were added to the indicated final concentrations either individually or together to assess their effects on the NanoLuc signal. As can be seen in Figure 4, these additions caused a dose-dependent decrease in the NanoLuc luminescence signal, indicating some detrimental interaction between the ionophores and the luciferase. At 220 s same amounts of purified SufI-Cpep86 was again added to determine whether the presence of the ionophores irreversibly hindered the interaction between 11S and SufI-Cpep86 in terms of NanoLuc assembly; it did not. Notably, ethanol alone caused a reproducible decrease in the NanoLuc signal (Fig. 4, *A*–*C*). Accordingly, we expressed in Figure 4*D* the inhibition of the NanoLuc signal as a percentage of the nigericin or valinomycin treatment relative to the ethanol treatment to remove the background effect of the solvent alone. A cutoff of 90% was used to assess whether the ionophore effect is significant (Fig. 4*D*). Valinomycin at a final concentration of 1 μM or higher exhibited a significantly negative impact on the NanoLuc signal, such that 1 μM brought the signal to ∼68%, and 2 μM lowered it to ∼48% relative to the positive ethanol control (Fig. 4, *A* and *D*). For nigericin, 10 μM dropped the signal to ∼43% of the ethanol treatment. Interestingly, 1 μM of nigericin appeared to minimally mitigate the effect of ethanol on the NanoLuc signal, such that it produced a value higher than 100% relative to the ethanol treatment (Fig. 4, *B* and *D*). While we do not currently know why these ionophores negatively affected the NanoLuc signal and did not pursue it further, we noted that their effects were minimal when their concentrations remained below 0.5 μM, separately or in combination, a concentration still expected to dissipate the PMF in spheroplasts.

In addition to nigericin or valinomycin directly affecting the NanoLuc signal, it is possible that they could also exhibit a negative impact on the synthesis of SufI-Cpep86 precursor, and this could also prevent the luminescence signal from increasing in the NanoLuc assay. Previous studies have shown that ionophores, including valinomycin and nigericin, mildly inhibited protein synthesis in *E. coli* but exhibited a stronger protein synthesis inhibition in the gram-positive bacteria *Staphylococcus aureus* which lacks outer membranes (31). Other studies have indicated that the *E. coli* outer membrane serves as a barrier against the entry of ionophores into the cell (32). Accordingly, we could not rule out the possibility that nigericin and valinomycin could inhibit protein synthesis in the *E. coli* spheroplasts as these are devoid of the outer membrane. In order to test this possibility, a spheroplast Tat transport assay was carried out in which we monitored the presence of both precursor and mature substrate (Fig. 5). IPTG was added to the wtTat spheroplasts to induce the expression of SufI-Cpep86 at 0 min, followed by the addition of ethanol (E), nigericin (N), or valinomycin (V), either individually or together. Transport reactions continued for the next 15 min before harvesting the spheroplasts. Both precursor and mature SufI-Cpep86 were observed in the ethanol treatment after 15 min, indicating successful protein induction and transport. However, neither mature nor precursor SufI-Cpep86 were observed after addition of low concentrations of nigericin or nigericin plus valinomycin, which suggests that nigericin strongly impedes the induction of protein synthesis. It should be noted that, although faint precursor bands were observed in the valinomycin treatment, these were not comparable to

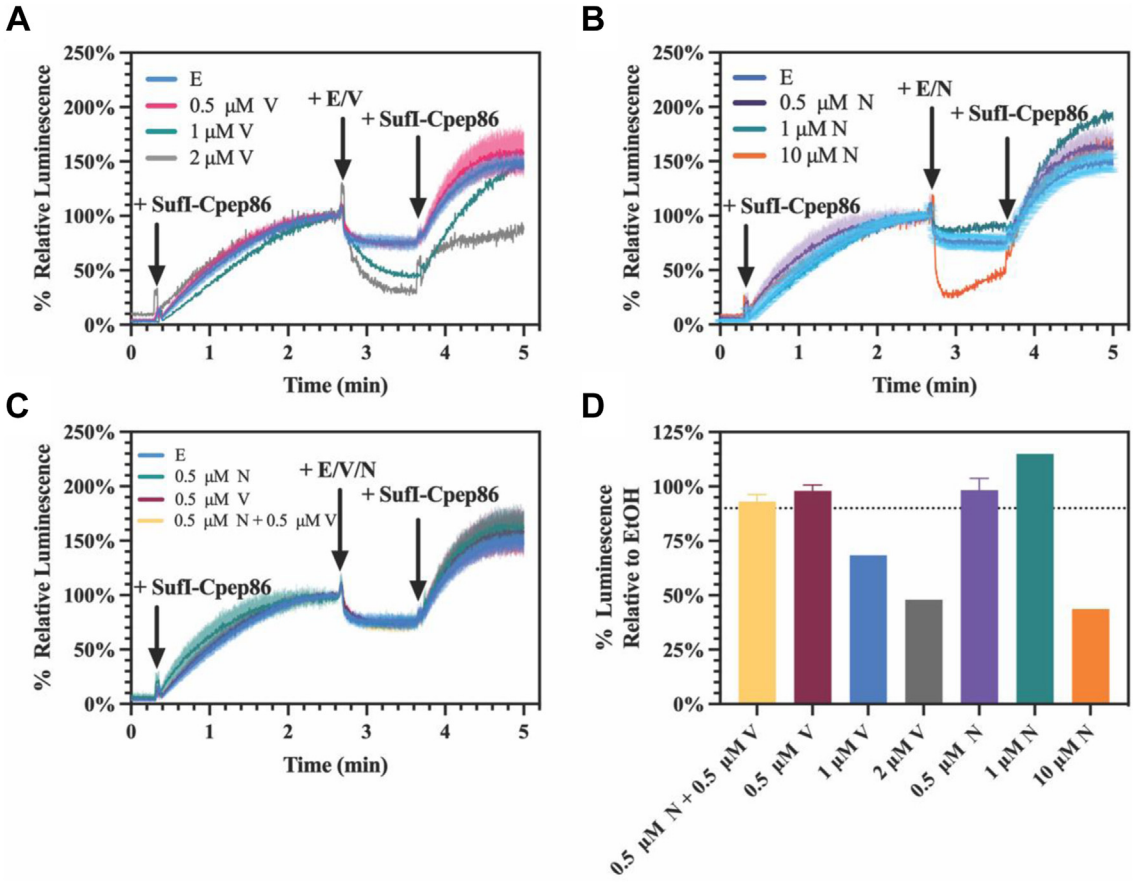

Figure 4. Effects of the ionophores on the NanoLuc signals in reconstitution *in vitro* without *Escherichia coli* spheroplasts. *A–C*, NanoLuc luminescence in the presence of ethanol (E), valinomycin (V), nigericin (N), or both ionophores (N + V) at the indicated final concentrations. Purified SufI-Cpep86 was added to a final concentration of 6.6 nM. *D*, bar plot showing the percent luminescence upon ionophores addition relative to the ethanol addition. A cutoff of 90% is denoted as *dotted line*. Experiments were performed at pH = 6.3. Error bars represent standard error among three technical replicates.

those observed with the ethanol treatment (Fig. 5*A*). Taken together, these results indicate that nigericin and valinomycin at concentrations above 0.5 μM negatively affect the synthesis of the SufI-Cpep86 protein precursor in *E. coli* spheroplasts. In this case, we could not distinguish whether a flattening in the luminescence signal in the NanoLuc assay upon ionophore addition (Fig. 3) was due to cessation of transport or to an inability of the cells to replenish the precursor protein.

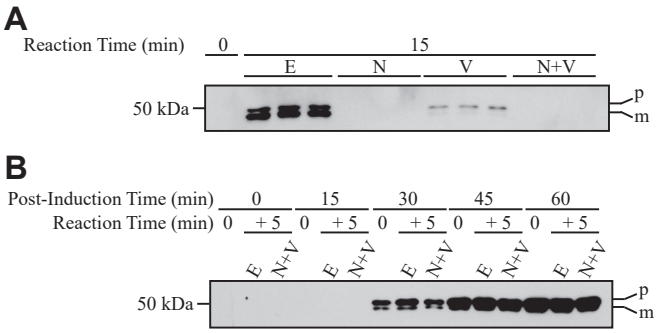

Figure 5. Effects of ionophores on protein synthesis. Total extracts of *Escherichia coli* spheroplasts expressing wtTat and FLAG-tagged SufI-Cpep86 were immunoblotted. *A*, ethanol or ionophores were added at 0 min and reactions continued for 15 min. Ethanol (E); 0.5 μM valinomycin (V); 0.5 μM nigericin (N); 0.5 μM of both ionophores (N + V). *B*, *top row* indicates the amount of time in minutes after IPTG induction. *Second row* indicates the time before ethanol or ionophores were added (*i.e.*, 0 min) and after the reaction (*i.e.*, 5 min). A representative immunoblot from three replicates is shown. Experiments were performed at pH = 6.3. Other details as in Figure 2.

In order to minimize the negative impact on protein synthesis upon ionophore addition, we needed to identify a time window for the experiment which satisfies the following criteria. First, sufficient amounts of SufI-Cpep86 precursor should be present throughout the measuring time window so that refilling of the precursor pool by new synthesis is not required. Second, the measuring time should be short enough that minimal changes occur in the total amount of precursor during the reaction. Upon fulfilling these conditions, the possibility that a lack of precursor leads to a flattening of the NanoLuc curve can be ruled out. To determine the optimal time window, IPTG was added to the wtTat spheroplast to initiate precursor synthesis at 0 min, followed by the addition of ethanol (E) or nigericin plus valinomycin (N + V) at t = 0, 15, 30, 45, and 60 min post-IPTG induction. The transport reactions were then continued for the next 5 min, after which the spheroplasts were harvested. We then compared the level of protein precursor before and after the various treatments. As seen in Figure 5*B*, detectable amounts of SufI-Cpep86 precursor were observed 30 min after IPTG induction. However, the overall amount of precursor present was rather low,

and it decreased in the 5 min after ionophore addition (compare lanes E and N + V at 30 min). However, after 45-min post induction, there is a minimal visual difference in the level of precursor protein between the E and N + V samples, and before the additions (Fig. 5*B*). Based on these results, we chose to monitor the transport reactions for 5 min at 45 min post induction as the optimal time for ionophore addition to ensure the presence of a sufficient amount of SufI-Cpep86 precursor.

Consequently, we modified the NanoLuc assay to incorporate these optimized conditions. To wit, the spheroplasts were incubated for 45 min after IPTG induction to allow the accumulation of an excess of precursor. Subsequently, spheroplasts were pelleted and resuspended to remove the accumulated mature SufI-Cpep86 transported out of the cells to the medium, which reduced the background signal (Fig. S1). Washed spheroplasts were resuspended with fresh 1× $M9^+$ medium, and then the NanoLuc assay was initiated. First, we performed the NanoLuc assay without further adjusting the pH of the medium (pH_{out} = 6.3). Ethanol (E), nigericin (N), valinomycin (V), or both ionophores (N + V) were added at 20 s. The curve for ethanol treatment continued to increase over the 5 min monitoring time, indicating continuous protein transport. Upon addition of both ionophores or valinomycin alone, the signal reached a plateau around 3.5 min, *i.e.*, the transport reaction stopped, consistent with the requirement for the Δψ for protein transport observed earlier (12). Notably, addition of nigericin alone also caused the transport reaction to stop, with the NanoLuc signal behaving as was observed when valinomycin was added; that is, transport stopped by approximately 3.5 min (Fig. 6*A*). Given that nigericin at concentrations as low as 0.05 μM have been observed to be sufficient to abolish the ΔpH in the outer membrane deficient *E. coli* cells with minimal compensation from Δψ (32), we expect that the 0.5 μM used in this experiment effectively dissipated the ΔpH in our spheroplasts. Considering the possibility that the change in the NanoLuc signals is an artefact of a significant change in the amount of spheroplasts present throughout the measurement, we compared the spheroplast-to-whole-cell ratio before and after the measurement using the spheroplast lysis method described in Materials and Methods (26). Regardless of the addition of ethanol or ionophores, the percentages of spheroplasts after the measurement averaged greater than 90% of the spheroplast percentages before the measurement (Fig. S2). Hence, it is unlikely that the significant changes observed upon the addition of ionophores are due to the changes in the number of spheroplasts present in the reaction. The immunoblot results in Figure 6, *C* and *D* are consistent with this conclusion, as majority of proteins present in the periplasmic fraction were in their mature forms, indicating that this is due to transport rather than spheroplast bursting during the measurement. Accordingly, the separate inhibition of Tat protein transport in *E. coli* by both nigericin and valinomycin indicates that this reaction is powered by both components of the PMF, as is the case for thylakoids (8).

To further examine the effects of nigericin on Tat transport in our experiments, we carried out the same NanoLuc assay at an elevated pH of 7.8 in the external medium. that is, closer to that of the cytoplasm (33). We reasoned that at this higher pH, the spheroplasts would be unable to develop a significant ΔpH between the cytoplasm and the periplasmic-like external medium. Under these conditions, we might expect the effect of nigericin to be minimal if its principal action in earlier experiments was to dissipate a ΔpH. Figure 6*B* shows that this was indeed the case. As in Figure 6*A*, at pH 7.8 (Fig. 6*B*) valinomycin, either alone or combined with nigericin, continued to cause cessation of the rise of the NanoLuc signal.

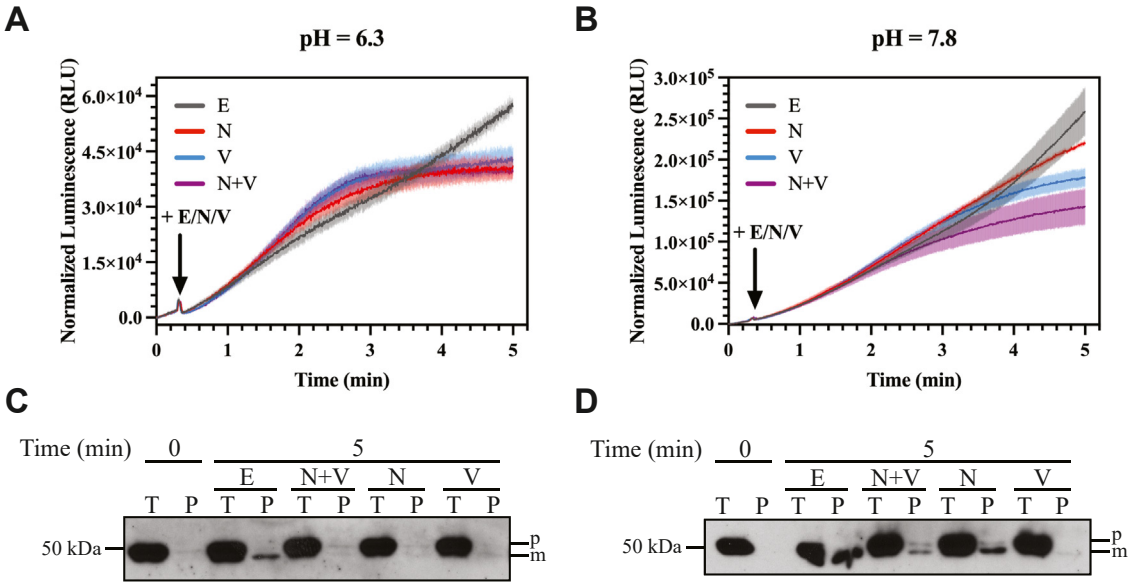

Figure 6. The NanoLuc assay reports a role for ΔpH in Tat transport in *Escherichia coli* spheroplasts. *A* and *B*, NanoLuc transport curves at pH = 6.3 (*A*) and pH = 7.8 (*B*). *Arrows* indicate addition of ethanol or ionophores. *Shades* represent the standard error from three replicates. E, ethanol; N, 0.5 μM of nigericin; V, 0.5 μM of valinomycin; N + V, 0.5 μM each nigericin and valinomycin. *C* and *D*, representative immunoblots of the samples taken at the beginning (0 min) and the end (5 min) of the NanoLuc assay at pH = 6.3 (*C*) and pH = 7.8 (*D*). T, total extract; P, periplasmic fraction (*i.e.*, supernatant); other details as in Figure 2. Three replicates were performed for each group. Other details as in Figure 2.

However, the effect of nigericin addition was greatly diminished at this pH. It is noteworthy that the luminescence produced by the recombined luciferase is significantly higher at pH 7.8 than at pH 6.3, which we expected due to our observed enhanced NanoLuc activity at higher pH (Fig. S3).

It is also possible that changes in pH can affect the rate of 11S-pep86 NanoLuc assembly, leading to change in the luminescence. However, it is not a concern in this study, as we aim to compare the transport kinetics among different treatments at the same pH rather than across different pH values. The rates of the assembly between the ionophore treatments and control should be the same at the same pH. Nonetheless, the relative slopes of the control curves were similar. We can conclude from this experiment that the effect of nigericin observed at pH 6.3 was due to its dissipation of the ΔpH and not an effect on the luciferase reaction.

We also examined by SDS-PAGE and immunoblotting the total cell extract and the periplasmic samples which were collected before and after these luminescence measurements. At pH 6.3, only the ethanol treatment exhibited a strong mature band (Fig. 6*C*), and valinomycin and nigericin both inhibited protein transport. At pH 7.8, nigericin caused much less inhibition of Tat transport (Fig. 6*D*), consistent with the idea that the ΔpH contributes only minimally to the PMF at this high pH. Additionally, the level of precursor present in the different treatments at the end of luminescence measurements were similar which was consistent with our previous results. Notably, we observed faint background bands of the precursor in the periplasmic samples. This may have been caused by a small amount of lysis of the spheroplasts during the measurement. However, the intensities of these precursor bands were much lower compared to the intensities of the bands observed with the ethanol-treated groups, which were the positive controls (Figs. 5*B*, and 6, *C* and *D*).

Taken together, our experiments show that we have modified the NanoLuc assay to faithfully report the transport kinetics *via* the Tat pathway in *E. coli* spheroplasts. Consistent with previous findings *in vitro* using *E. coli* IMVs (12), dissipation of the bulk PMF by adding nigericin and valinomycin, together, as well as dissipation of the Δψ alone, using valinomycin, abolishes Tat transport. However, we observed that ΔpH also plays a role in the Tat transport in *E. coli* spheroplasts *in vivo* using the NanoLuc assay. Tat transport was stopped when the proton gradient was dissipated by nigericin under the conditions where a significant ΔpH (pH_{out} = 6.3) was present. It follows then that the energetics of the Tat pathway in bacteria is not substantially different from that in thylakoids, relying on both components of the PMF.

Discussion

In order to achieve a better understanding of the Tat transport mechanism, a continuous assay to monitor the transport with high resolution is desirable. Lack of such an assay makes it difficult to investigate Tat transport kinetics in a comprehensive manner. Current quantitative assays in investigation of the Tat transport *in vivo*, such as pulse-chase experiments, requires a series of complex procedures and relies on fitting with a regression model to estimate the transport kinetics (11). Here, we describe and validate a novel luminescence Tat transport assay utilizing the split-NanoLuc luciferase system to monitor the Tat transport kinetics *in vivo*. Merits of the NanoLuc assay include the following considerations: First, by using *E. coli* spheroplasts as the experimental platform, the Tat transport is assessed *in vivo*, under nearly native conditions. Second, since the Tat machinery transports proteins in their folded conformations, disruption of the original conformation upon tag addition to the Tat substrate should be minimized or avoided. This is achieved with the NanoLuc complement pep86 (10 aa), where its impact on the overall conformation of the Tat substrate is expected to be relatively small. Third, the sensitive and continuous nature of the NanoLuc assay allows us to observe the transient and subtle changes in transport upon the application of treatments during the reaction time course. Fourth, the NanoLuc assay involves relatively few steps compared to conventional pulse-chase experiments and *in vivo* transport assays, minimizing sample handling. While our results, and previous studies (18, 21), indicate that pH and several ionophores have a direct effect on the NanoLuc signals (Figs. 4 and S3), we were able to manage these effects by optimization of the assay. Altogether, our results indicate that the NanoLuc assay is a convenient and accurate measure of Tat transport activity.

The energy requirement of the Tat transport system in both bacteria and chloroplasts has been studied for decades (8, 12, 30). In plants, ΔpH is the dominant driving force for Tat transport across the thylakoid membrane (30, 34, 35). This is likely because thylakoids generally partition most of their PMF as a ΔpH, although a substantial Δψ can be developed under some conditions, both *in vivo* and *in vitro* (36). Indeed, thylakoids can utilize the Δψ to drive Tat protein transport, and accordingly, the thylakoid PMF is considered to power this process (8). In contrast to this, it has been suggested that the Δψ, but not ΔpH, drives Tat protein transport in *E. coli* (12). This was surprising given that the Tat pathway has long been thought to operate by a conserved mechanism in both plants and bacteria (1).

We recognized that our new luminescence assay for Tat transport in *E. coli* affords us a new opportunity to examine the energetics of this process in bacteria *in vivo*. Under our conditions and using *E. coli* spheroplasts, we report that the ΔpH, in addition to the Δψ, plays a role in the Tat transport. When a significant ΔpH was allowed to develop by electron transport, dissipation of the proton gradient using nigericin resulted in a rapid abolishment of Tat transport. Similarly, and as has been reported earlier with *in vitro* studies (12), addition of valinomycin also lead to inhibition of Tat transport, confirming the role of the Δψ as a driving force (Fig. 6, *A* and *C*). Our results, which indicate that both ΔpH and Δψ play a role in Tat transport, unifies the PMF-dependency of the Tat transport in both thylakoids and bacteria. It should be noted that previous studies used *E. coli* IMVs as the experimental platform (12). It is possible that the different results may be due in part to the size difference between the membrane vesicles (∼100 nm in diameter) and *E. coli* spheroplasts

(~1 μm in diameter), and the resulting much smaller periplasmic volume in IMVs (37, 38).

In our experience, and as was already noted in the study of Bageshwar and Musser, we find it difficult to assess the energetic parameters operating during the entirety of the Tat transport reaction in IMVs. Addition of NADH to IMVs permits a measurement of the developed ΔpH and Δψ for only a few minutes until the reaction vessel is depleted of oxygen. However, the Tat transport reaction continues after components of the PMF can no longer be detected (12). While we cannot measure ΔpH or Δψ in spheroplasts, we do recognize that the energetic profile in living cells could be distinctly different than in IMVs. In particular, even if the spheroplast reaction vessel were to go anaerobic during the experiment, we could expect the PMF driving force for Tat transport to be maintained by reverse proton pumping by the EF1/EF0 ATPase using glycolysis-derived ATP. Furthermore, taking the possible compensation in Δψ upon nigericin addition into account, we have optimized the concentration of nigericin used in this study (0.5 μM), which is within the range (0.05–2 μM) found to be sufficient to dissipate the ΔpH in *E. coli* but to leave the Δψ remain relatively unchanged (32). Still, we observed that Tat transport stopped when ΔpH was dissipated by nigericin at pH = 6.3, suggesting a role of ΔpH in the Tat transport (Fig. 6, *A* and *C*). Interestingly, we observed that it requires around 2 min for the transport to completely stop, and we do not have a clear explanation for this phenomenon. To further support these observations, we performed the same set of experiment at the elevated pH of 7.8, where the environmental pH is close to the *E. coli* cytoplasmic pH (33). We found that addition of nigericin had minimal effect on the Tat transport under these conditions (Fig. 6, *B* and *D*), ruling out the possibility that Tat transport was stopped by nigericin at pH 6.3 due to some nonspecific effect of the protonophore. Notably, the inhibitory effect of nigericin shown in Figure 6*D* appears to be more severe than that observed in Figure 6*B*. This is likely due to the loss of some mature protein due to sample handling, which is a drawback of the conventional immunoblot-based assay. Nevertheless, we are left with the conclusion that the ΔpH contributes to the driving force for Tat transport in *E. coli in vivo*.

To summarize, we have examined bacterial Tat transport energetics *in vivo* using our novel high-resolution real-time assay with the NanoLuc split-luciferase system. Our experiments clearly demonstrate that both Δψ and ΔpH can contribute to the driving force for Tat transport, suggesting that this reaction is powered by the PMF. Accordingly, we propose that there is no need to consider that this enigmatic transporter operates by different principles or different mechanisms in the several domains of life where it is found.

Experimental procedures

Strain and plasmid construction

E. coli strain DADE-A (MC4100, *ΔtatABCE*) was used in in both *in vivo* transport assay and the luminescence assay (39). The plasmid pTat101 (pTH19Kr derivative, a low copy plasmid constitutively expressing the TatABC) (40) was used for Tat expression. *ΔtatA*, the TatA knockout variant, was produced by QuikChange site-directed mutagenesis (New England BioLabs, Phusion High-Fidelity PCR Kit) followed by KLD (Kinase, Ligase, and DpnI) digestion (New England BioLabs) by using primers deltaTatA_F (5′-GTGTTTGATATCGGTTTTAGC-3′) and deltaTatA_R (5′-GGATCCTCCTCTGTGGTA-3′). pep86 was introduced at the relevant position of the pQE80l (SufI-FLAG) by QuikChange site directed mutagenesis followed using the following primers: Npep86_F (5′-CCTGTTTAAAAAAATTGGCTCCGGCTCACTCAGTCGGCGT-3′) and Npep86_R (5′- CGCCAGCCGCTCACCATGGTTAATTTCTCCTCTTTAATGAATTCTG-3′) for N-terminal addition; Cpep86_F (5′- GCGCCTGTTTAAAAAAATTTAAGTCGACCTGCAGCCA-3′) and Cpep86_R (5′- CAGCCGCTCACGCCGGAGCCCTTATCGTCGTCATCCTTGTAATC -3′) for C-terminal addition. For the pCDFduet (His-11S) construct, 11S was synthesized with NdeI and XhoI restriction enzyme recognition sites and inserted into an empty pCDFduet under the control of the T7 promoter. 6× His tag was introduced by QuikChange mutagenesis using Nhis11S_F (5′-CATGGCGTCTTCACCCTGGAAGAC-3′) and Nhis11S_R (5′-GTGATGGTGACCCATATGTATATCT-3′). All constructs were confirmed by Sanger sequencing.

In vivo *transport assay*

Plasmids pTat101 or *ΔtatA* were cotransformed with pQE80l (SufI-FLAG), pQE80l (Npep86-SufI-FLAG), or pQE80l (SufI-Cpep86-FLAG), which is under the control of the T5 promoter, into the Tat knockout strain, DADE-A. Details of the *in vivo* transport assay was described elsewhere (28). Overnight cultures were diluted into the fresh LB medium. 1 mM IPTG was added for induction of SufI and SufI-pep86 variants when the A_{600} of the cell culture reached 0.5. Cells were continuously cultured at 37 °C for another 2.5 h before proceeding to cellular fractionation.

Protein expression and purification

6× His-tagged 11S was cloned into the expression vector pCDFduet (Fig. 1*C*) and transformed into BL21 (λDE3). When A_{600} reached 0.7, proteins were overexpressed overnight at 4 °C upon induction with IPTG induction at a final concentration of 0.25 mM. Cells were placed on ice for 10 min before being centrifuged at 10,000 g for 10 min at 4 °C. Proteins were purified under native conditions by Ni-NTA chromatography in the following steps (12). Pellets were resuspended on ice in lysis buffer (25 mM *N*-cyclohexyl-3-aminopropanesulfonic acid, pH = 9, 250 mM NaCl, 20 mM imidazole, and 0.2% Triton X-100) to obtain a 50× concentrated cell lysate. Lysates were sonicated followed by centrifugation at 10,000 rpm (Beckman JA-14) for 25 min at 4 °C. Subsequently, for 10 ml cell lysates, 2.5 ml of the 50% Ni-NTA (Qiagen) slurry was added and gently mixed on a rotary shaker at 4 °C for 1 h. The resin was then loaded onto a 10 X 3 cm column. The following buffers were added sequentially (1): 15 ml wash buffer 1 (100 mM tricine, pH = 8, 1 M NaCl, 20 mM imidazole,

and 0.2% Triton X-100) (2); 15 ml wash buffer 2 (10 mM tricine, pH = 8, 100 mM NaCl, and 10 mM imidazole) (3); 5 ml wash buffer 3 (10 mM tricine, pH = 8, 100 mM NaCl, 10 mM imidazole, and 50% glycerol). 6× His-tagged proteins were eluted by adding 12 ml of elution buffer (100 mM NaCl, 250 mM imidazole, pH = 8.0, and 50% glycerol) and collected as 2-mL fractions. Buffer exchange was performed to exchange the elution buffer with protein storage buffer (50 mM Tris–HCl, pH = 8, 100 mM KCl, and 10% glycerol) using Amicon centrifugal filter units (MilliporeSigma) for long-term storage at −80 °C. Protein concentrations were estimated by measuring the absorbance at 280 nm and by SDS-PAGE.

Preparation of the E. coli *spheroplast*

Plasmids pTat101 or *ΔtatA* were cotransformed with pQE80l (SufI-Cpep86-FLAG) into the DADE-A strain (39). Overnight bacterial cultures were grown in LB medium supplemented with 0.4% glucose to suppress the expression of SufI-Cpep86. The next day, these cultures were diluted in fresh LB medium supplemented with 0.4% glucose at a ratio of 1:33 and grown at 37 °C until the A_{600} reached 0.6 to 0.9. Preparation of spheroplast was derived from the protocol from Schäfer *et al.* (41). All centrifugations were performed at 5000 rpm (Beckman JA-14) for 10 min at 4 °C. 200 ml of the cells with OD_{600} equivalent to 1.0 were centrifuged and resuspended with 45 ml of resuspension buffer (100 mM Tris-HCl, pH = 7.5, 0.5 M sucrose). Cells were converted to spheroplast by adding an equal volume of spheroplast-converting buffer (8 mM EDTA, pH = 8.0, 0.01 mg/ml lysozyme) and incubation on ice for 10 min. Assessment of the conversion percentage was carried out by calculating the ratio of A_{600} of the samples diluted with double distilled water to the ones diluted by osmotic-stabilizing 1× $M9^+$ medium (1× M9 medium diluted from 5× M9 salt, supplemented with 0.1 mM $CaCl_2$, 0.002% thiamine, 2 mM $MgSO_4$, 0.01% of the 20 amino acids, 2% glycerol as the carbon source, and 0.25 M sucrose) both at the ratio of 1:10. Since the spheroplasts lyse in double distilled water but not in 1× $M9^+$ medium, this calculation yields the fraction of the cells remaining unconverted (26). The typical conversion rate from whole cell to spheroplast using this method was above 90%. The spheroplasts were centrifuged and washed with 1× $M9^+$ medium once to remove the residual EDTA and lysozyme. Washed pellets were resuspended with 5 ml of 1× $M9^+$ medium and the A_{600} of the spheroplast mixture was measured. The concentrated spheroplast solution was incubated on ice and ready for use.

Tat NanoLuc transport assay

The real-time standard luminescence assays were carried out at 37 °C in a Jobin Yvon Fluorolog (Horiba) fluorimeter with the excitation lamp turned off. The luminescence was measured with the emission wavelength set at 460 nm with the slits open with a 10 nm bandpass. The reaction mixture, with the total volume of 2 ml, was assembled in a 3.5 ml standard cuvette with a stir bar and contained the following components: concentrated spheroplast solution in 1× $M9^+$ medium added to the final A_{600} of 1.0, 50 nM His-11S, 2.5 μl furimazine (Promega), with the addition of 1× $M9^+$ medium to a 2 ml volume. After equilibrating for 5 min, the luminescence baseline was measured. IPTG was then added after 50 s to a final concentration of 1 mM. After a measurement for either 400 s or 600 s, the ionophore dissolved in ethanol or ethanol, alone, was added to the reaction mixture as indicated, and luminescence was continuously measured until completion of the reaction.

For the experiments in investigation of the Tat energetics, *E. coli* spheroplasts were diluted in 1× $M9^+$ medium to the final A_{600} of 0.5. The spheroplast premix was incubated at 37 °C with continuous stirring for 5 min. IPTG was added to the final concentration of 1 mM. Spheroplasts were then incubated for 45 min with stirring. The transport reaction was then paused by incubation on ice. Spheroplasts were washed by centrifugation at 5000 rpm (Beckman JA-14) for 10 min at 4 °C to remove the excess transported SufI-Cpep86 in the periplasmic-like medium. Fresh 1× $M9^+$ medium was used to resuspend the spheroplasts to the final A_{600} of 0.5. The reaction mixture was prepared in the same manner as described above. Without further incubation, ethanol or ionophores were added after 20 s. Luminescence was then measured continuously for 5 min.

Cellular fractionation

For samples from the *in vivo* transport assay, 3 ml of cells with the A_{600} equivalent to 1.0 were harvested. A total cell extract was collected by resuspending 0.3 ml of cells with an A_{600} = 1.0 in 2× Laemmli sample buffer. For the isolation of the periplasmic fraction, cells were fractionated using the EDTA/lysozyme/cold osmotic shock method described above (42). The periplasmic fraction was solubilized by adding an equal volume of 2× Laemmli sample buffer prior to SDS-PAGE.

For samples from the luminescence assay, samples were taken prior to the addition of treatment and at the end of the reaction. Transport was stopped by immediately placing the samples on ice. The total spheroplast extract was collected and the samples were centrifuged at 16,000*g* for 2 min at 4 °C. The supernatant was collected as the periplasmic-like fraction (P) and solubilized by mixing with 4× Laemmli sample buffer (Bio-Rad). The pellet was resuspended with the same volume of the 1× M9+ medium and solubilized with 4× Laemmli sample buffer. All samples were heated at 80 °C for 3 min and subsequently subjected to SDS-PAGE and immunoblotting.

SDS-PAGE and immunoblotting

Samples were subjected to SDS-PAGE. Upon transfer onto polyvinylidene fluoride membranes and blocking, an α-FLAG (GenScript) monoclonal antibody was used to probe for FLAG-tagged SufI or FLAG-tagged SufI-pep86 followed by a horseradish peroxidase-conjugated α-mouse antibody (Santa Cruz Biotechnology Inc). Labeled proteins were visualized using either ProSignal Pico or ProSignal Femto ECL Western Blotting detection kit (Prometheus).

Data analysis

Raw NanoLuc luminescence readouts were normalized using RStudio (Ver. 1.4.1103). For calculating the percentage of luminescence, the luminescence reading obtained immediately before treatment addition was set as 100% (*i.e.*, the luminescence reading baseline signal). Relative luminescence was defined by the difference between the raw luminescence signal and the baseline signal. For the calculation of the relative luminescence values, the luminescence reading baseline was calculated by averaging the signal in the first 20 s. Normalized data sets were imported into GraphPad Prism version 9.3.0 for macOS (GraphPad Software, www.graphpad.com), where graphs were generated and annotated.

Data availability

All data are contained within the manuscript.

Supporting information—This article contains supporting information.

Author contributions—W. Z., B. H., T. M. B., and S. M. T. conceptualization; W. Z., B. H., T. M. B., and S. M. T. methodology; W. Z., B. H., T. M. B., and S. M. T. writing–review and editing; W. Z. and B. H. investigation; W. Z., B. H., and S. M. T. writing–original draft; S. M. T. supervision; S. M. T. funding acquisition.

Funding and additional information—We gratefully acknowledge support from the Division of Chemical Sciences, Geosciences, and Biosciences, Office of Basic Energy Sciences of the US Department of Energy through Grant DE-SC0020304 to S. M. T.

Conflict of interest—The authors declare that they have no conflicts of interest with the contents of this article.

Abbreviations—The abbreviations used are: IMV, inverted membrane vesicle; NanoBiT, NanoLuc Binary Technology; PMF, Protonmotive force; Tat, twin arginine translocation.

References

1. Berks, B. C. (2015) The twin-arginine protein translocation pathway. *Annu. Rev. Biochem.* **84**, 843–864
2. Hutcheon, G. W., and Bolhuis, A. (2003) The archaeal twin-arginine translocation pathway. *Biochem. Soc. Trans.* **31**, 686–689
3. Robinson, C., and Bolhuis, A. (2004) Tat-dependent protein targeting in prokaryotes and chloroplasts. *Biochim. Biophys. Acta Mol. Cell Res.* **1694**, 135–147
4. Aldridge, C., Spence, E., Kirkilionis, M. A., Frigerio, L., and Robinson, C. (2008) Tat-dependent targeting of Rieske iron-sulphur proteins to both the plasma and thylakoid membranes in the cyanobacterium Synechocystis PCC6803: Tat-dependent protein targeting in cyanobacteria. *Mol. Microbiol.* **70**, 140–150
5. Bachmann, J., Bauer, B., Zwicker, K., Ludwig, B., and Anderka, O. (2006) The Rieske protein from Paracoccus denitrificans is inserted into the cytoplasmic membrane by the twin-arginine translocase. *FEBS J.* **273**, 4817–4830
6. Berks, B. C., Palmer, T., and Sargent, F. (2005) Protein targeting by the bacterial twin-arginine translocation (Tat) pathway. *Curr. Opin. Microbiol.* **8**, 174–181
7. Palmer, T., and Berks, B. C. (2012) The twin-arginine translocation (Tat) protein export pathway. *Nat. Rev. Microbiol.* **10**, 483–496
8. Braun, N. A., Davis, A. W., and Theg, S. M. (2007) The chloroplast Tat pathway utilizes the transmembrane electric potential as an energy source. *Biophys. J.* **93**, 1993–1998
9. Fröbel, J., Rose, P., and Müller, M. (2012) Twin-arginine-dependent translocation of folded proteins. *Philosophical. Trans. R. Soc. B: Biol. Sci.* **367**, 1029–1046
10. Theg, S. M., Cline, K., Finazzi, G., and Wollman, F.-A. (2005) The energetics of the chloroplast Tat protein transport pathway revisited. *Trends Plant Sci.* **10**, 153–154
11. Stanley, N. R., Palmer, T., and Berks, B. C. (2000) The twin arginine consensus motif of Tat signal peptides is involved in Sec-independent protein targeting in Escherichia coli. *J. Biol. Chem.* **275**, 11591–11596
12. Bageshwar, U. K., and Musser, S. M. (2007) Two electrical potential-dependent steps are required for transport by the Escherichia coli Tat machinery. *J. Cell Biol.* **179**, 87–99
13. Barrett, C. M. L., Ray, N., Thomas, J. D., Robinson, C., and Bolhuis, A. (2003) Quantitative export of a reporter protein, GFP, by the twin-arginine translocation pathway in Escherichia coli. *Biochem. Biophys. Res. Commun.* **304**, 279–284
14. Thomas, J. D., Daniel, R. A., Errington, J., and Robinson, C. (2001) Export of active green fluorescent protein to the periplasm by the twin-arginine translocase (Tat) pathway in Escherichia coli. *Mol. Microbiol.* **39**, 47–53
15. DeLisa, M. P., Samuelson, P., Palmer, T., and Georgiou, G. (2002) Genetic analysis of the twin arginine translocator secretion pathway in bacteria. *J. Biol. Chem.* **277**, 29825–29831
16. Ize, B., Stanley, N. R., Buchanan, G., and Palmer, T. (2003) Role of the Escherichia coli Tat pathway in outer membrane integrity: AmiA and AmiC are Tat substrates. *Mol. Microbiol.* **48**, 1183–1193
17. England, C. G., Ehlerding, E. B., and Cai, W. (2016) NanoLuc: a small luciferase is brightening up the field of bioluminescence. *Bioconjug. Chem.* **27**, 1175–1187
18. Dixon, A. S., Schwinn, M. K., Hall, M. P., Zimmerman, K., Otto, P., Lubben, T. H., *et al.* (2016) NanoLuc complementation reporter optimized for accurate measurement of protein interactions in cells. *ACS Chem. Biol.* **11**, 400–408
19. Allen, W. J., Watkins, D. W., Dillingham, M. S., and Collinson, I. (2020) Refined measurement of SecA-driven protein secretion reveals that translocation is indirectly coupled to ATP turnover. *Proc. Natl. Acad. Sci. U. S. A.* **117**, 31808–31816
20. Oh-hashi, K., and Hirata, Y. (2020) Elucidation of the molecular characteristics of wild-type and ALS-linked mutant SOD1 using the NanoLuc complementation reporter system. *Appl. Biochem. Biotechnol.* **190**, 674–685
21. Pereira, G. C., Allen, W. J., Watkins, D. W., Buddrus, L., Noone, D., Liu, X., *et al.* (2019) A high-resolution luminescent assay for rapid and continuous monitoring of protein translocation across biological membranes. *J. Mol. Biol.* **431**, 1689–1699
22. Needs, H. I., Lorriman, J. S., Pereira, G. C., Henley, J. M., and Collinson, I. (2023) The MitoLuc assay system for accurate real-time monitoring of mitochondrial protein import within mammalian cells. *J. Mol. Biol.* **435**, 168129
23. Allen, W. J., Corey, R. A., Watkins, D. W., Oliveira, A. S. F., Hards, K., Cook, G. M., *et al.* (2022) Rate-limiting transport of positively charged arginine residues through the Sec-machinery is integral to the mechanism of protein secretion. *eLife* **11**, e77586
24. Tsirigotaki, A., De Geyter, J., Šoštarić, N., Economou, A., and Karamanou, S. (2017) Protein export through the bacterial Sec pathway. *Nat. Rev. Microbiol.* **15**, 21–36
25. Black, P. N., Said, B., Ghosn, C. R., Beach, J. V., and Nunn, W. D. (1987) Purification and characterization of an outer membrane-bound protein involved in long-chain fatty acid transport in Escherichia coli. *J. Biol. Chem.* **262**, 1412–1419
26. Treptow, N. A., and Shuman, H. A. (1985) Genetic evidence for substrate and periplasmic-binding-protein recognition by the MalF and MalG

proteins, cytoplasmic membrane components of the Escherichia coli maltose transport system. *J. Bacteriol.* **163**, 654–660
27. Sargent, F., Berks, B. C., and Palmer, T. (2010) The Tat protein export pathway. *EcoSal Plus*. https://doi.org/10.1128/ecosalplus.4.3.2
28. Hao, B., Zhou, W., and Theg, S. M. (2022) Hydrophobic mismatch is a key factor in protein transport across lipid bilayer membranes *via* the Tat pathway. *J. Biol. Chem.* **298**, 101991
29. Stanley, N. R., Findlay, K., Berks, B. C., and Palmer, T. (2001) Escherichia coli strains blocked in Tat-dependent protein export exhibit pleiotropic defects in the cell envelope. *J. Bacteriol.* **183**, 139–144
30. Cline, K., Ettinger, W. F., and Theg, S. M. (1992) Protein-specific energy requirements for protein transport across or into thylakoid membranes. Two lumenal proteins are transported in the absence of ATP. *J. Biol. Chem.* **267**, 2688–2696
31. Alonso, M. A., Vázquez, D., and Carrasco, L. (1979) Compounds affecting membranes that inhibit protein synthesis in yeast. *Antimicrob. Agents Chemother.* **16**, 750–756
32. Ahmed, S., and Booth, I. R. (1983) The use of valinomycin, nigericin and trichlorocarbanilide in control of the protonmotive force in Escherichia coli cells. *Biochem. J.* **212**, 105–112
33. Krulwich, T. A., Sachs, G., and Padan, E. (2011) Molecular aspects of bacterial pH sensing and homeostasis. *Nat. Rev. Microbiol.* **9**, 330–343
34. Alder, N. N., and Theg, S. M. (2003) Protein transport *via* the cpTat pathway displays cooperativity and is stimulated by transport-incompetent substrate. *FEBS Lett.* **540**, 96–100
35. Mould, R. M., and Robinson, C. (1991) A proton gradient is required for the transport of two lumenal oxygen-evolving proteins across the thylakoid membrane. *J. Biol. Chem.* **266**, 12189–12193
36. Cruz, J. A., Sacksteder, C. A., Kanazawa, A., and Kramer, D. M. (2001) Contribution of electric field ($\Delta\psi$) to steady-state transthylakoid proton motive force (pmf) *in Vitro* and *in Vivo*. Control of pmf parsing into $\Delta\psi$ and ΔpH by ionic strength. *Biochemistry* **40**, 1226–1237
37. Eriksson, H. M., Wessman, P., Ge, C., Edwards, K., and Wieslander, Å. (2009) Massive Formation of intracellular membrane vesicles in Escherichia coli by a monotopic membrane-bound lipid glycosyltransferase. *J. Biol. Chem.* **284**, 33904–33914
38. Figueroa, D. M., Wade, H. M., Montales, K. P., Elmore, D. E., and Darling, L. E. O. (2018) Production and visualization of bacterial spheroplasts and protoplasts to characterize antimicrobial peptide localization. *JoVE*. https://doi.org/10.3791/57904
39. Wexler, M., Sargent, F., Jack, R. L., Stanley, N. R., Bogsch, E. G., Robinson, C., *et al.* (2000) TatD is a cytoplasmic protein with DNase activity. No requirement for TatD family proteins in sec-independent protein export. *J. Biol. Chem.* **275**, 16717–16722
40. Kneuper, H., Maldonado, B., Jäger, F., Krehenbrink, M., Buchanan, G., Keller, R., *et al.* (2012) Molecular dissection of TatC defines critical regions essential for protein transport and a TatB–TatC contact site. *Mol. Microbiol.* **85**, 945–961
41. Schäfer, U., Beck, K., and Müller, M. (1999) Skp, a molecular chaperone of gram-negative bacteria, is required for the formation of soluble periplasmic intermediates of outer membrane proteins. *J. Biol. Chem.* **274**, 24567–24574
42. Petiti, M., Houot, L., and Duché, D. (2017) Cell fractionation. In: Journet, L., Cascales, E., eds. *Bacterial Protein Secretion Systems: Methods and Protocols*, Methods in Molecular Biology, Springer, New York, NY: 59–64. https://doi.org/10.1007/978-1-4939-7033-9_3